Chapter 4

Results and Disscussion

4.1 Adsorbent Selection

The characteristics of YAO, PHO and HRO activated carbon were represented in Table 4.1. and in Figure 4.1.

Table 4.1: The characteristics of YAO, PHO and HRO.

Activated Carbon	Characteristics		
	Surface Area(cm^2/g)		Avg. Pore Diameter (Å)
	BET	Langmuir	
YAO	1.39×10^7	1.85×10^7	14.79
PHO	1.01×10^7	1.35×10^7	14.77
HRO	9.58×10^6	1.28×10^7	14.72

As could be seen, all of these activated carbon have almost the same characteristics. With the highest surface area, YAO has been the selected adsorbent in the present study. In addition, the morphology of the external surface of YAO was studied by Scanning Electron Microscopy (SEM). A typical micrograph was illustrated in Figure 4.2.

It is apparent that the external surface of this carbon was quite rough, consisting of cavities, cracks and irregular protrusions.

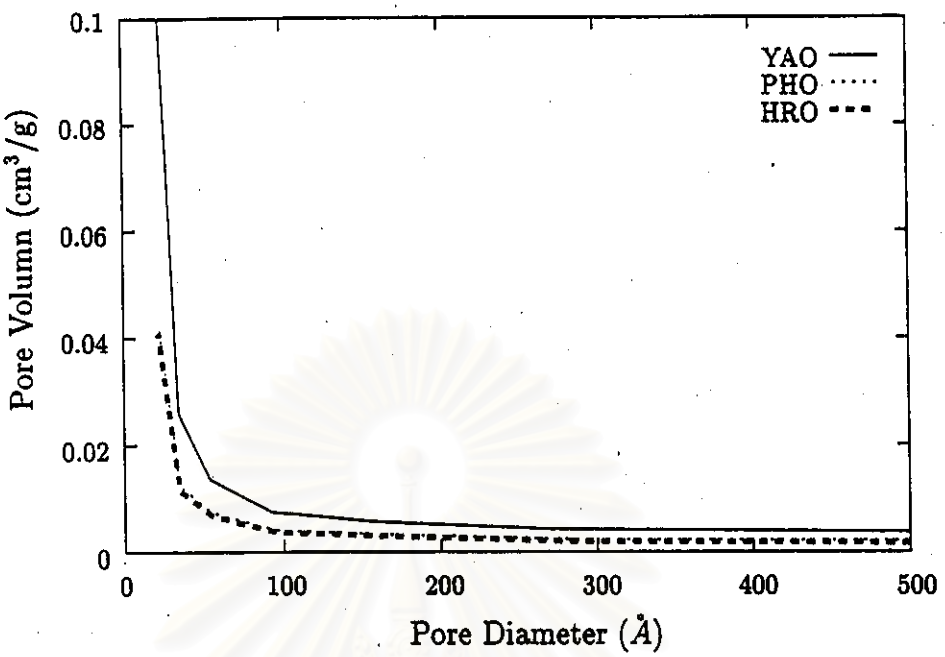

Figure 4.1: Pore size distribution of YAO, PHO and HRO.

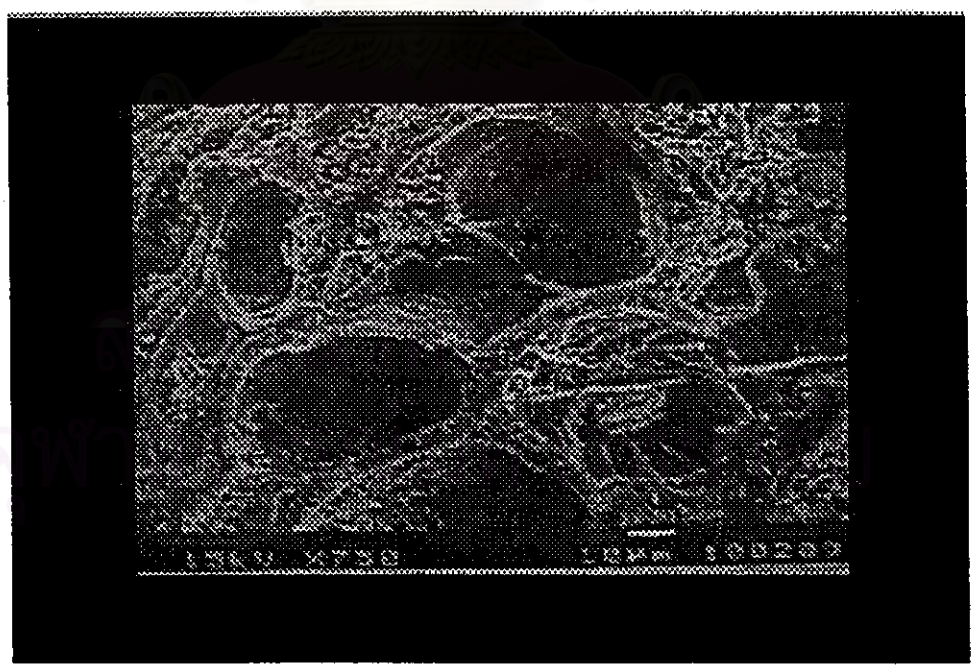

Figure 4.2: Scanning electron micrograph of the external surface of YAO.

4.2 Adsorption Isotherm of Acetylene on YAO at 323 K

For 20%V/V of acetylene in feed with superficial velocity 15 cm/s, the breakthrough concentration from 8 cm long bed of 60-80 mesh YAO has reached the same value as that of the feed for a period of 60 sec at least, as illustrated in Figure 4.3. Therefore, the amount adsorbed can be determined from the difference

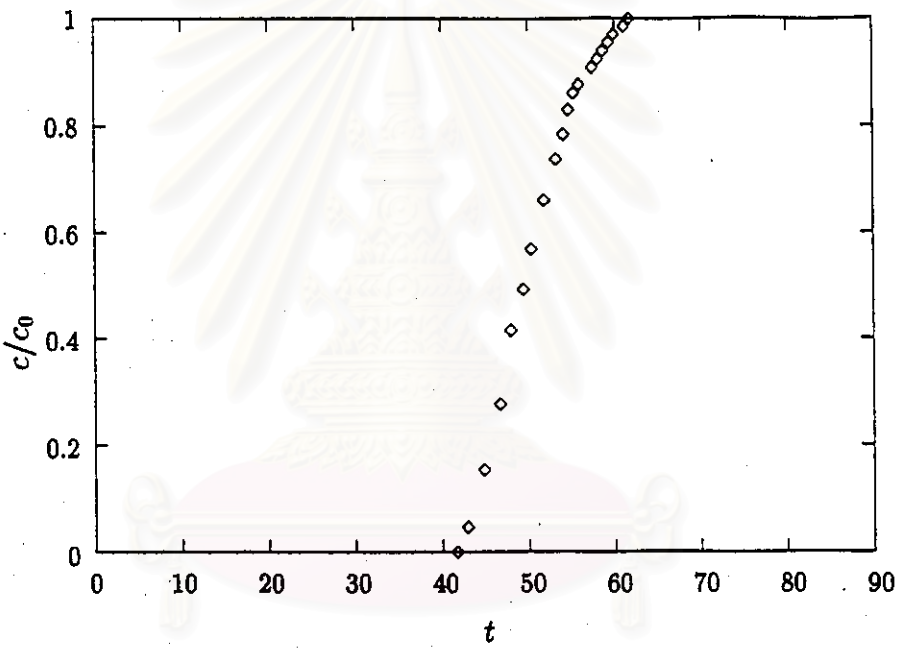

Figure 4.3: An experimental breakthrough curve of 20%V/V acetylene in feed with superficial velocity 15 cm/s from 8 cm long bed of YAO

between the total feed amount and the sum of the total amount breakthroughed the adsorber and the total amount accumulated in gas phase in the adsorber for that period. The calculation method is represent in Appendix A. In addition, the amount adsorbed has been determined for the velocity 5 cm/s. It has been found that the acetylene amount adsorbed for both velocity are equal. Consequently, it

may assume that the adsorption equilibrium can be achieved within the 8 cm long packed column of YAO with the velocity 15 cm/s. Subsequently, the adsorbed amount of acetylene is in equilibrium with the partial pressure of acetylene in the adsorber. Then, the equilibrium amount adsorbed at various partial pressures can be obtained, as summarized in Table 4.2.

Table 4.2: Adsorption equilibrium data of acetylene on YAO at 323 K.

Acetylene Concentration		Adsorption Capacity, q
%V/V	Partial pressure (kPa)	(mmol/g)
13.06	25.76	1.99
13.44	31.51	2.44
19.89	39.24	2.65
20.26	47.48	3.03
26.65	52.75	3.23
26.75	62.46	3.34
33.3	66.04	3.59
33.48	78.04	3.81
39.74	78.39	4.05
39.86	93.41	4.36
46.57	98.61	4.73
49.99	104.96	4.85
53.21	105.64	4.90
53.56	109.21	4.94
53.7	117.92	5.05
59.78	118.92	5.26
60.29	125.86	5.30
60.41	131.06	5.53
66.44	131.50	5.64
66.56	141.58	5.82
66.67	144.03	5.87
73.02	144.83	5.88
73.43	155.99	5.93
73.53	157.53	6.05

The equilibrium is non-linear. With Langmuir model, a plot of $1/q$ with respect to $1/P$ has yielded a straight line, as shown in Figure 4.4.

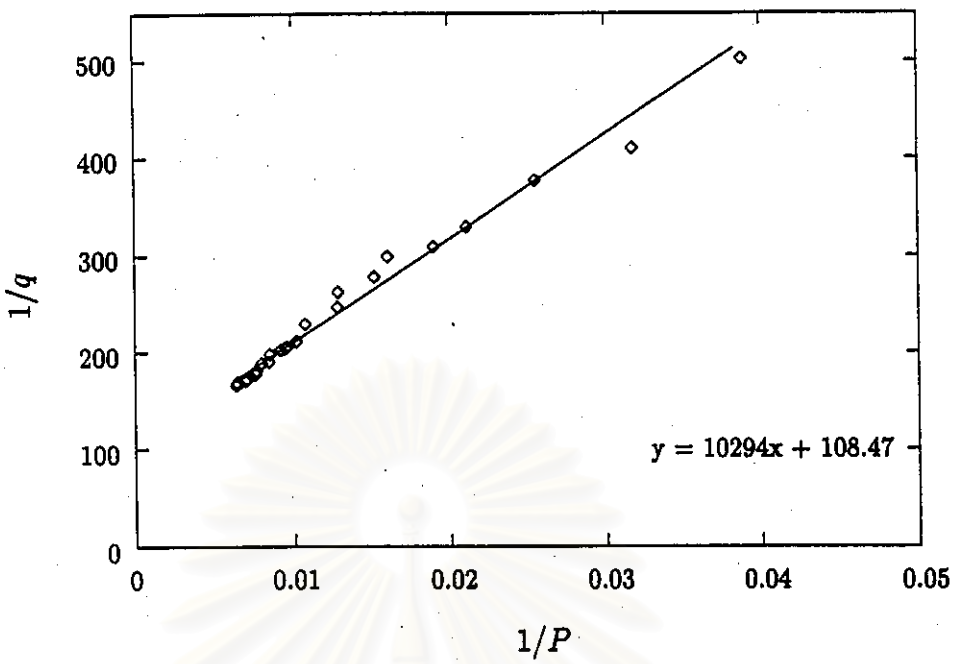

Figure 4.4: An experimental equilibrium plot with the Langmuir model.

This linear relationship of $1/q$ with $1/P$ can be written as

$$\frac{1}{q} = \frac{1}{q_s} + \frac{1}{K_L q_s}\frac{1}{P} \tag{4.1}$$

Thus, the maximum amount adsorbed, q_s, can be determined from the intercept. While the Langmuir constant, K_L, is obtained from the slope of the line. Both adsorption parameters are summarized in Table 4.3.

Table 4.3: Langmuir parameters.

Langmuir Parameters	
K_L (kPa^{-1})	1.05×10^{-2}
q_s (mmol/g)	9.2

Alternatively, it may assume that the equilibrium has agreed with Freudlich model. Therefore, the plot of q with respect to P in log-log scale has yieled a

straight line, as well, as shown in Figure 4.5.

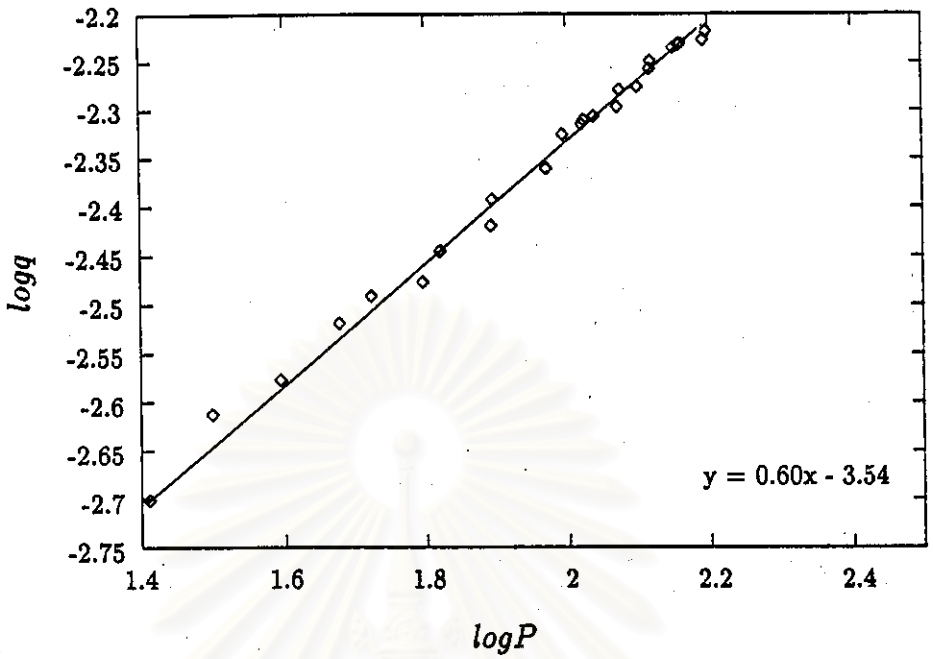

Figure 4.5: An experimental equilibrium plot with the Freudlich model.

Similarly, the Freudlich constant, K_F, and the constant, n, can be determined from the intercept and the slope of the line, respectively, as summarized in Table 4.4.

Table 4.4: Freudlich parameters.

Freudlich Parameters	
K_F (kPa^{-1})	2.90×10^{-3}
n	1.65

In addition, both Langmuir and Freudlich models have been compared with the experimental data in Figure 4.6.

Furthermore, the agreement between these two models and the experimental data have been verified by the normalized root mean square (%RMS), which is

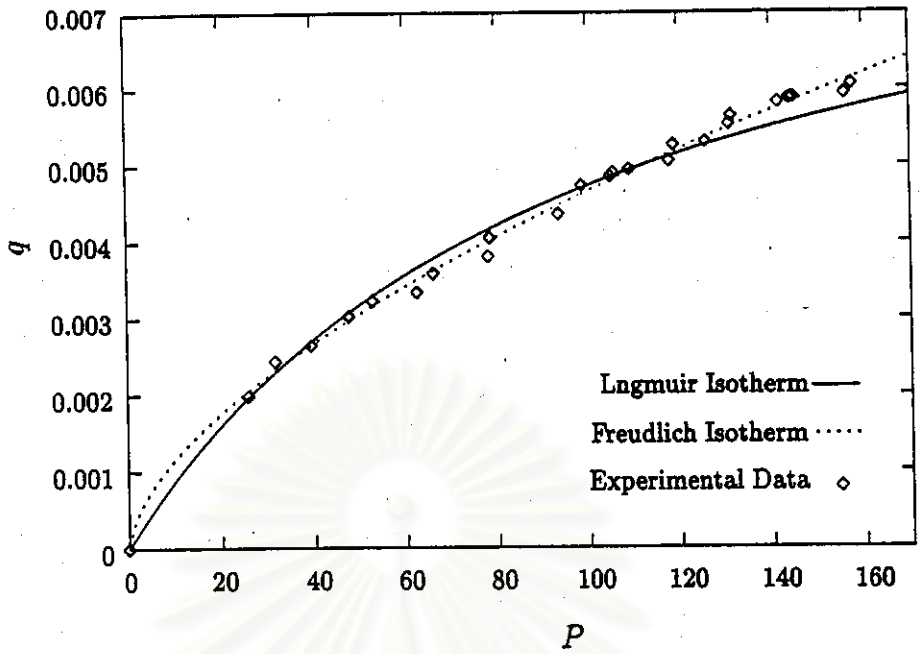

Figure 4.6: The comparison between the experimental equilibrium data, Langmuir model and Freudlich model.

evaluated from the following equation 4.2 [25].

$$\%RMS = \sqrt{\frac{1}{N_{pt}} \sum_{i=1}^{N_{pt}} \left(\frac{q_{exp} - q_{cal}}{q_{exp}} \right)^2} \times 100 \qquad (4.2)$$

The results are represented in Table 4.5.

Table 4.5: A normalrize root mean square.

Isotherm Model	%RMS
Langmuir	4.20
Freudlich	2.58

It has been observed that, Freudlich model yielded an excellent overall fit. While, Langmuir model deviate considerably from the experimental data at high concentrations and slightly less at low concentrations. Therefore, Freudlich parameters was selected for further used.

In addition, the experimental data have been compared with the publish results obtained from static volumetric method in Figure 4.7 [26]. However, these results

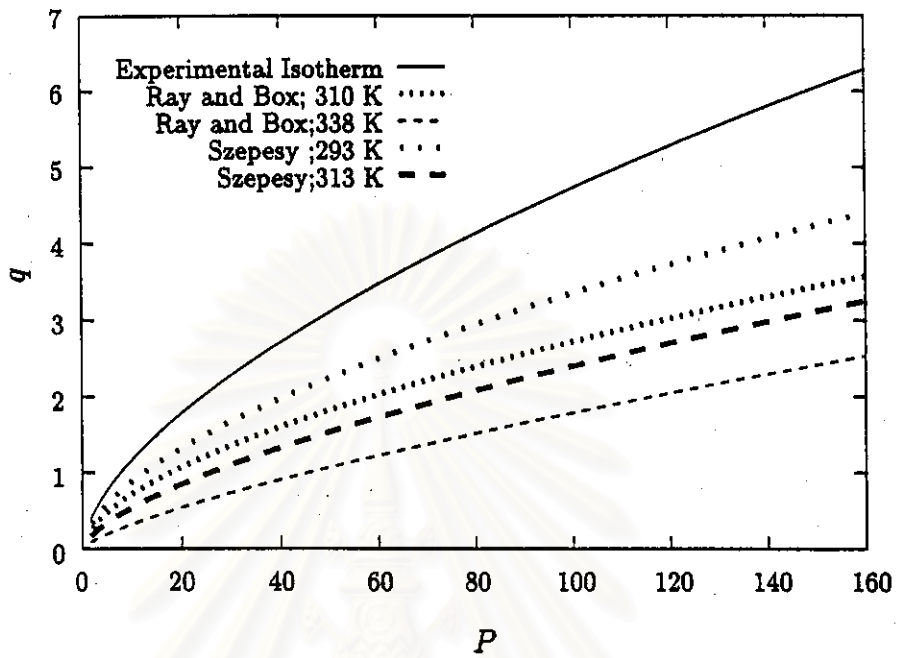

Figure 4.7: The comparison between the experimental equilibrium data and the publish results.

do not generally provide experimental data of the same activated carbon and at the same temperature.

Ray and Box used Columbia grade L activated carbons, 1.15×10^{-7} cm^2/g,in their experiments whereas Szepesy used Nuxit-L activated carbons, 1.10×10^{-7} cm^2/g. The present data are consistantly higher than the others, which may be due to the highest specific surface area of YAO, 1.85×10^{-7} cm^2/g. This increase in the surface area results in a tremendous difference in the equlibrium capacity of the adsorbent. Interestingly, however, Columbia and Nuxit had about the same specific surface area, the data of Ray and Box are obviosly different

from those of Szepesy even though their experiment were performed at almost the same temparature. Therfore, the equilibrium data are highly dependent on the type of activated carbon used. [11]. Futhermore, the present experiment were performed in different enviroment than the reference experiment because helium was presented.

4.3 Dynamic Variation of Concentration Profiles

The concentration profile at the breakthrough time can be obtained from the breakthrough results. For L_1 cm long bed, the breakthrough time, t_{bL_1} is defined as the time at the dimensionless concentration of 0.05. The average prapagation velocity at any dimensionless concentration, $w_{L_1,c/c_0}$, can be determined from

$$w_{L_1,c/c_0} = \frac{L_1}{t_{L_1,c/c_0}} \tag{4.3}$$

where $t_{L_1,c/c_0}$ is the time at the corresponding dimensionless concentration.

Based on the average propagation velocity, the axial position at the breakthrough time, $S_{L_1,c/c_0}$, can be approcimated from

$$S_{L_1,c/c_0} = w_{L_1,c/c_0} t_{bL_1} \tag{4.4}$$

For L_2 cm long bed ($L_2 > L_1$), the axial position of the corresponding dimesionless concentration is determined from the axial position of L_1 cm long bed and the average propagation rate of acetylene within an additional bed, expressed as

$$S_{L_2,c/c_0} = S_{L_1,c/c_0} + \left(\frac{L_2 - L_1}{t_{L_2,c/c_0} - t_{L_1,c/c_0}}\right)(t_{bL_2} - t_{bL_1}) \tag{4.5}$$

The examples of calculation are represented in Appendix A.

4.3.1 Effects of Bed Length

For the 20%V/V acetylene with the velocity of 15 cm/s, the concentration profile in the bed containing 60-80 mesh YAO tends to disperse towards the exit end as an increase in bed length, as illustrated in Figure 4.8. For the concentration

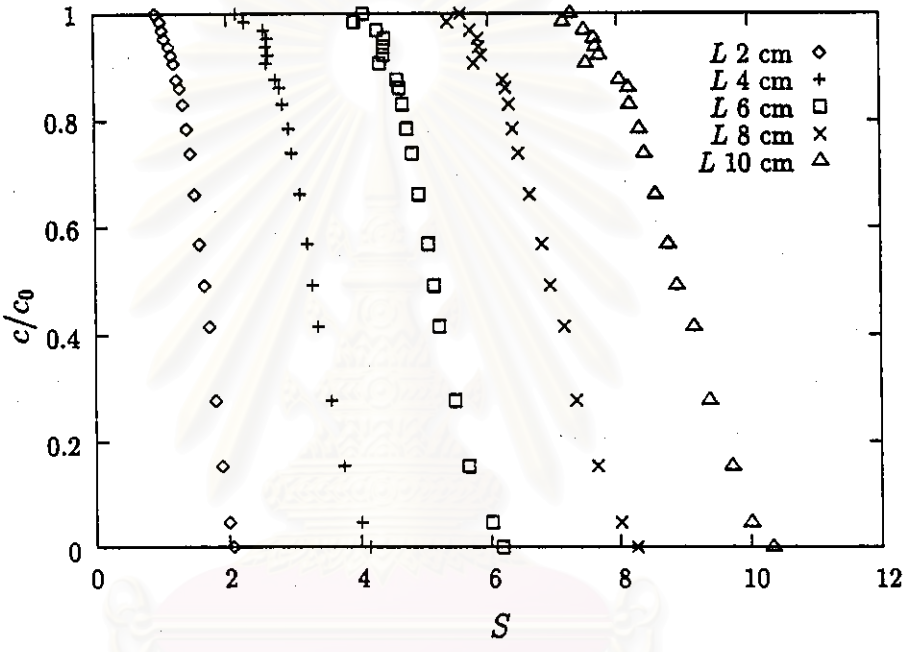

Figure 4.8: The concentration profile of acetylene 20%V/V at the superficial velocity of 15 cm/s

of 33%V/V and 60%V/V, the variations of the concentration profile with the bed length are similar to that of the concentration of 20%V/V, as shown in Figure 4.9. These demonstrate that the leading region of the concentration profile does not reach the equilibrium immediatly. Under the circumstances, the amount adsorbed may be much less than the amount which is in equilibrium with the concentration

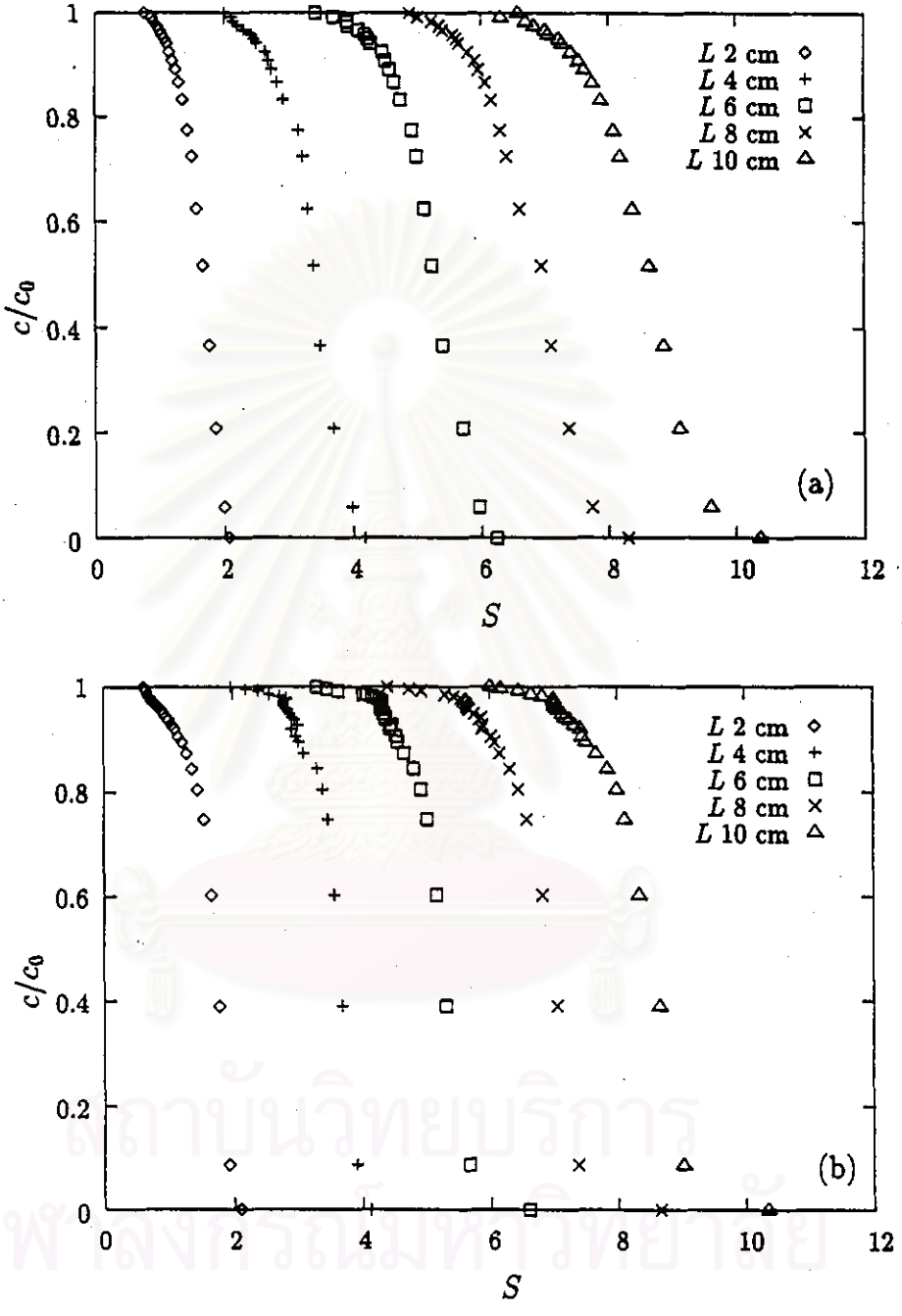

Figure 4.9: The concentration profiles of acetylene at the superficial velocity of 15 cm/s : (a) 33%V/V, (b) 60%V/V.

in the gas phase at the corresponding axial positions. Consequently, the maximum bed length of these experiments is still less than the minimum bed length for established the constant shape concentration profile.

In order to verify the effects of axial dispersion on the shape of the concentration profile, similar experiments on an unpacked column and a sand packed column of 6 cm length have been carried out additionally. The concentration profiles of acetylene correspond with the step change at the feed end, as illutrated in Figure 4.10. Without adsorption, the axial dispersion does not effect the shape of the concentration profile in both columns. Therefore, only the finite rate of mass transfer affects the shape of the profile.

4.3.2 Effects of Particle Sizes of YAO

For a 6 cm long beds of 40-60 mesh YAO and of 30-40 mesh YAO, the concentration profiles of 20%V/V fed acetylene are compared with that in the bed of 60-80 mesh YAO, as shown in Figure 4.11.

Under the circumstances, the particle sizes of YAO do not affect the shape of the concentration profile. With 33%V/V and 60% acetylene in the feed, the particle sizes of YAO also do not affect the shape of the profiles, as illustrated in Figure 4.12. These demonstrate that the rates of adsorption on these particles are in the same order of magnitudes.

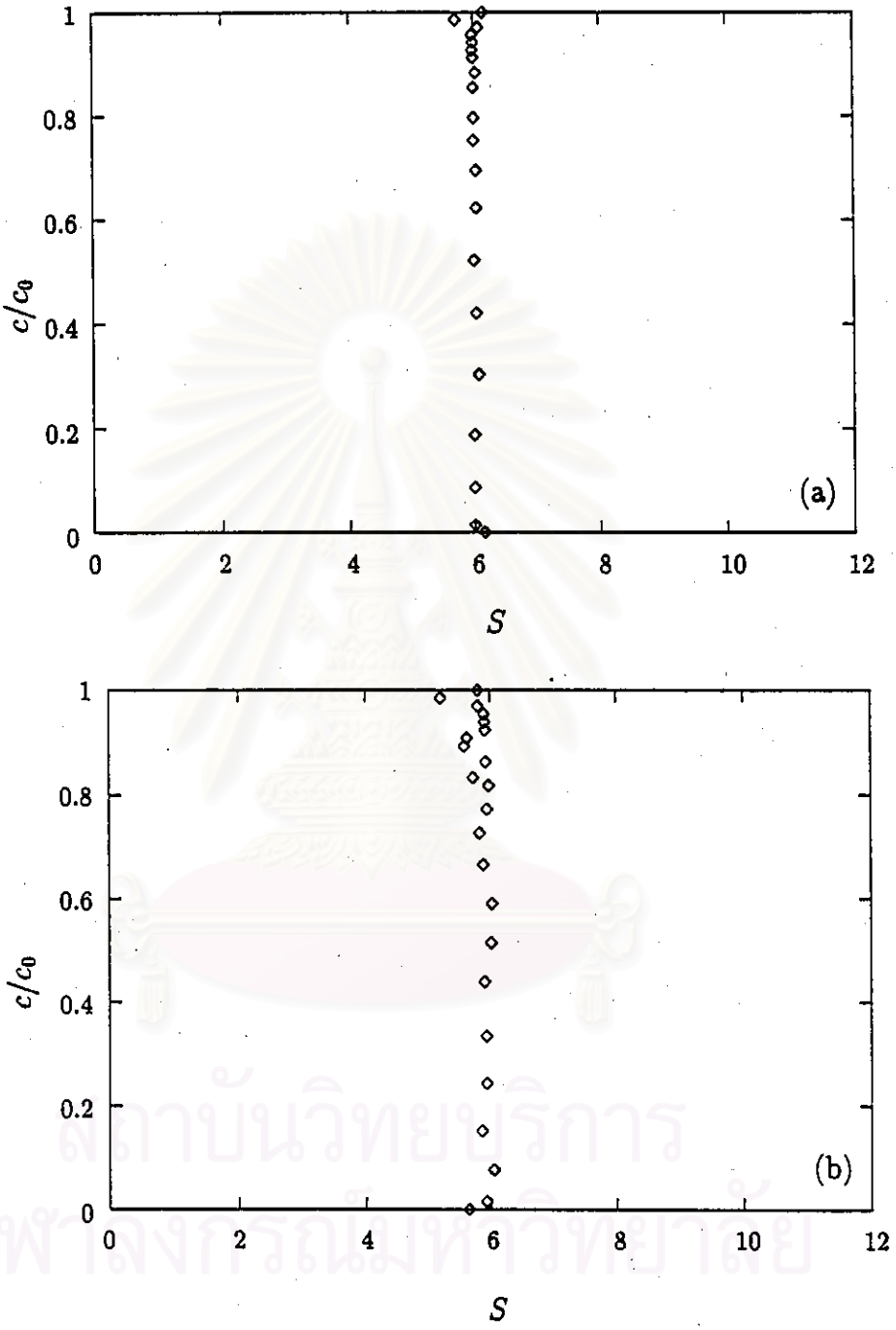

Figure 4.10: The concentration profiles of acetylene at superficial velocity of 15 cm/s : (a) unpacked column, (b) sand packed column.

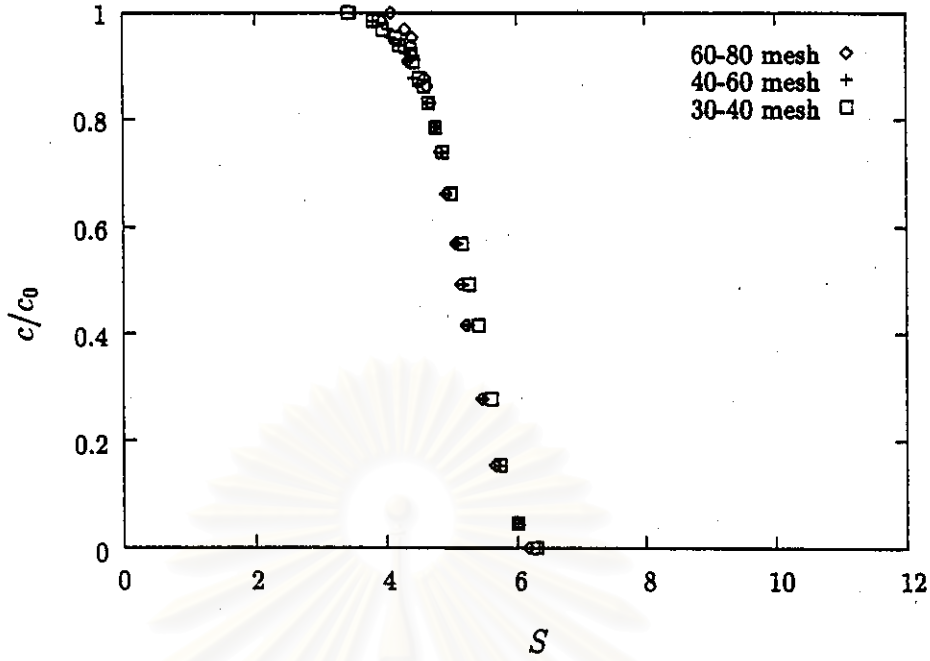

Figure 4.11: The concentration profile of acetylene 20%V/V using 60-80, 40-60 and 30-40 mesh YAO.

4.3.3 Effects of Superficial Velocities

- **Effects of Velocities on the Shapes of the Profile**

For the 6 cm long bed of YAO, the shape of the concentration profile disperses longitudinally as an increase in the superficial velocities, as shown in Figure 4.13. These demonstrates an increase in the effects of convective mass transfer. On the contrary, the dispersion of the profile is reduced by decreasing the velocity. At the velocity of 5 cm/s, the shape of the profile approaches the step shange in the concentration at the feed end. In other words, the convective mass transfer hardly affects on the shape of the profile.

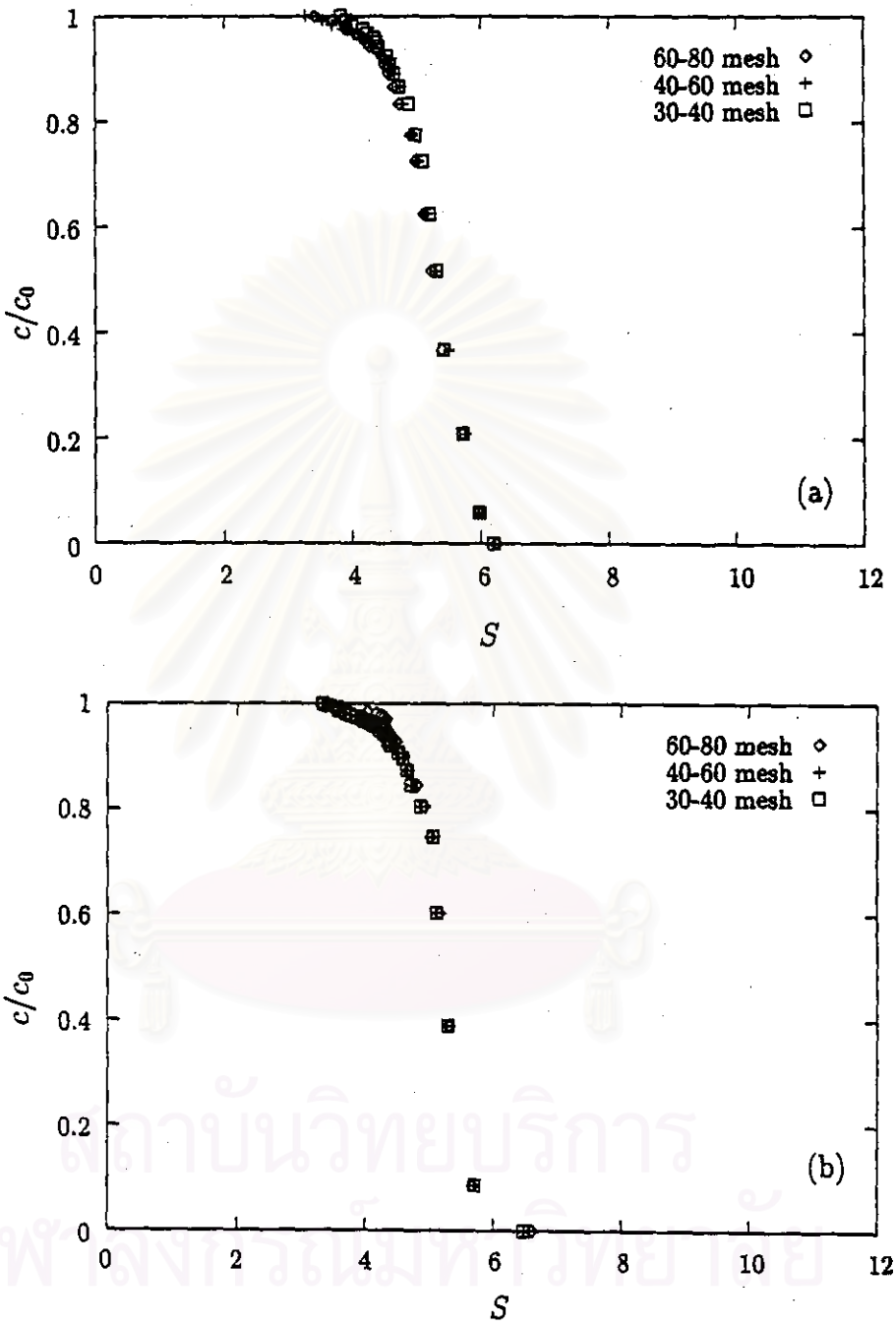

Figure 4.12: The concentration profile of acetylene using 60-80, 40-60 and 30-40 mesh YAO : (a) 33%V/V, (b) 60%V/V.

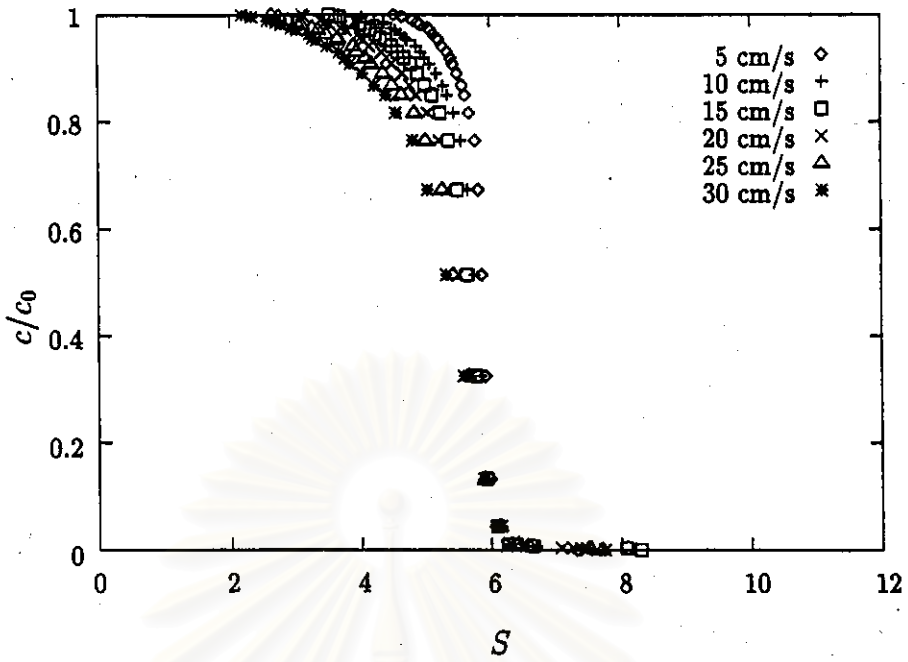

Figure 4.13: The concentration profile of acetylene 60%V/V at superficial velocity 5, 10, 15, 20, 25 and 30 cm/s.

- **Effects of Velocities on the Propagation of the Profile**

By reducing the superficial velocity from 15 cm/s to 5 cm/s, the shape of concentration profile of 20%V/V acetylene tends to be constant after passing the bed length of 4 cm, as shown in Figure 4.14. For 33%V/V and 60%V/V acetylene in the bed, the shapes of the profiles tend to unchange as propagating through the bed length of 4 cm, as well, as illustrated in Figure 4.15. Under the circumstances, the leading region of the profile has approached the equilibrium within an approxiate period, as shown in Figure 4.16. Since the mean residence time for the velocity of 15 cm/s is much less than that for the velocity 5 cm/s, the leading region of the profile will reaches the equilibrium in a bed of larger length than 10 cm.

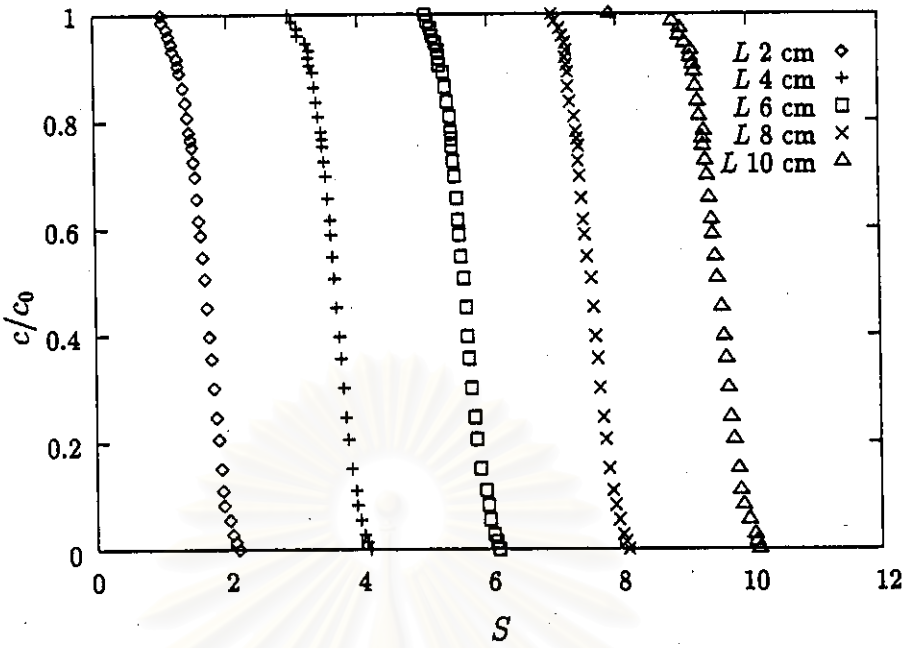

Figure 4.14: The concentration profile of acetylene 20%V/V at the superficial velocity of 5 cm/s.

Figure 4.16 also illustrates that the gaseous mixture of a high concentration can propagate within the bed faster than that of a low concentration. These phenomena correspond with the effects of the adsorption isotherm on the shape of the concentration profile.

4.4 Variation of the Mass Transfer Zone

As acetylene propagates through the YAO bed with various length, the variation of the shape of the concentration profile may be determined quantitatively with the length of the mass transfer zone (MTZ). Theoretically, the MTZ is a region in which the concentration just rises from the initial concentration, usually being zero, to the immediate feed concentration. Therefore, the length of the MTZ

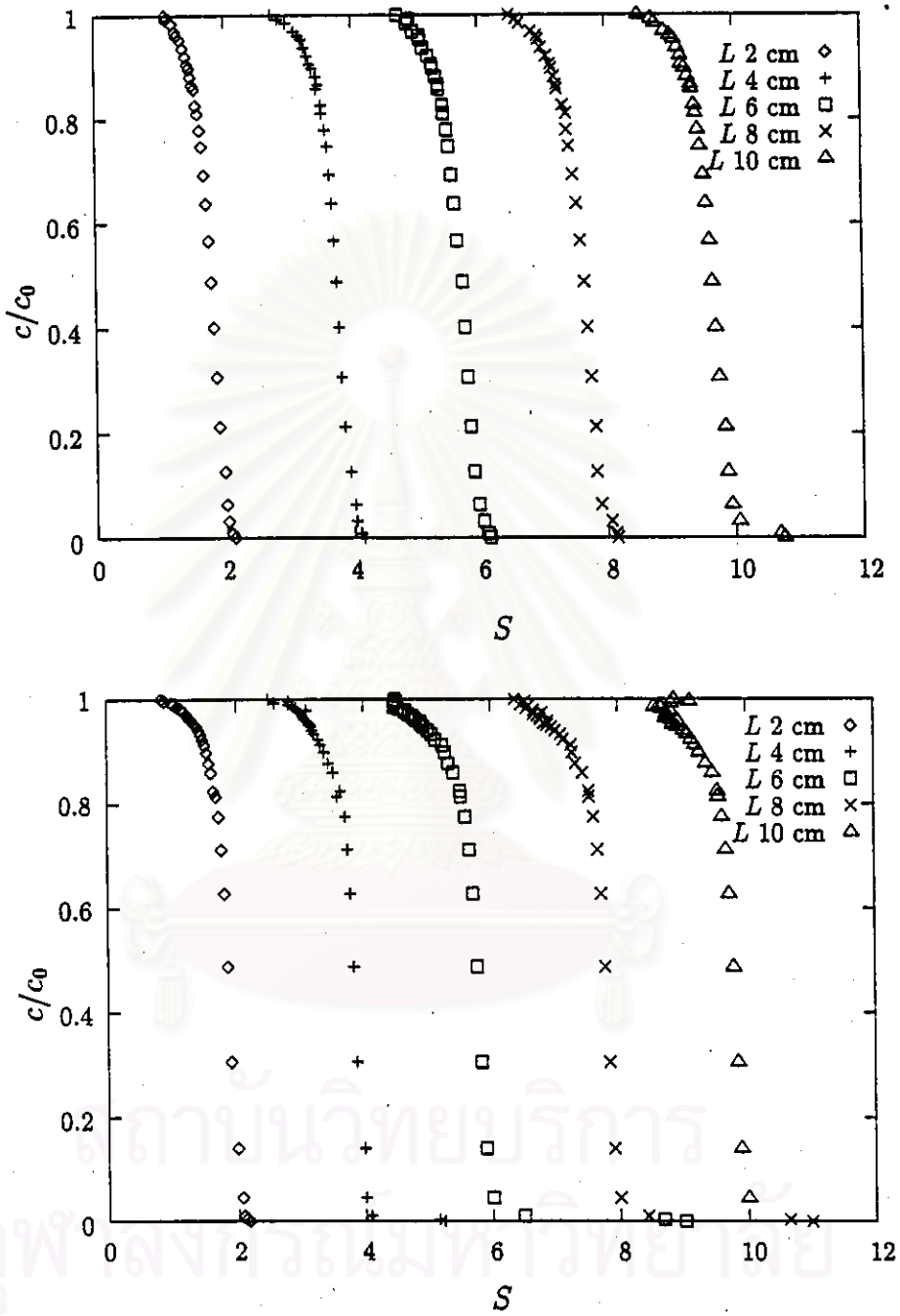

Figure 4.15: The concentration profile of acetylene at the superficial velocity of 5 cm/s : (a) 33%V/V, (b) 60%V/V.

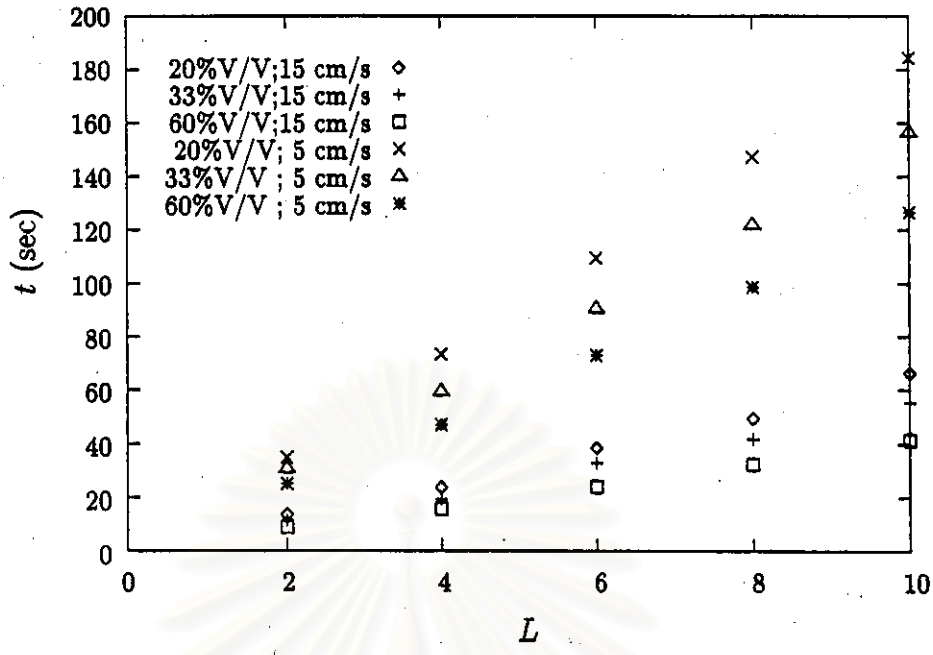

Figure 4.16: Mean residence time of experimental breakthrough curve.

is equal to the axial distance between the just rise concentration and the immediate feed concentrationof the corresponding concentration profile. In practice, the MTZ length, however, is usually determined from the distance between 5% to 95% feed concentration of the corresponding profile. In this work, the MTZ length is defined as the distance between the 10% to 90% feed concentration instead.

The MTZ lengths of all experiments illustrated in Figure 4.17.

For the velocity of 15 cm/s, the MTZ length of each feed concentration increases as an increase in the bed length. Since the high concentration of acetylene can propagate through the bed faster than that with low concentration, the MTZ length of 60%V/V acetylene, is shorter than of the others for a given bed length.

While the MTZ lengths of all feed concentration with the velocity of 5 cm/s

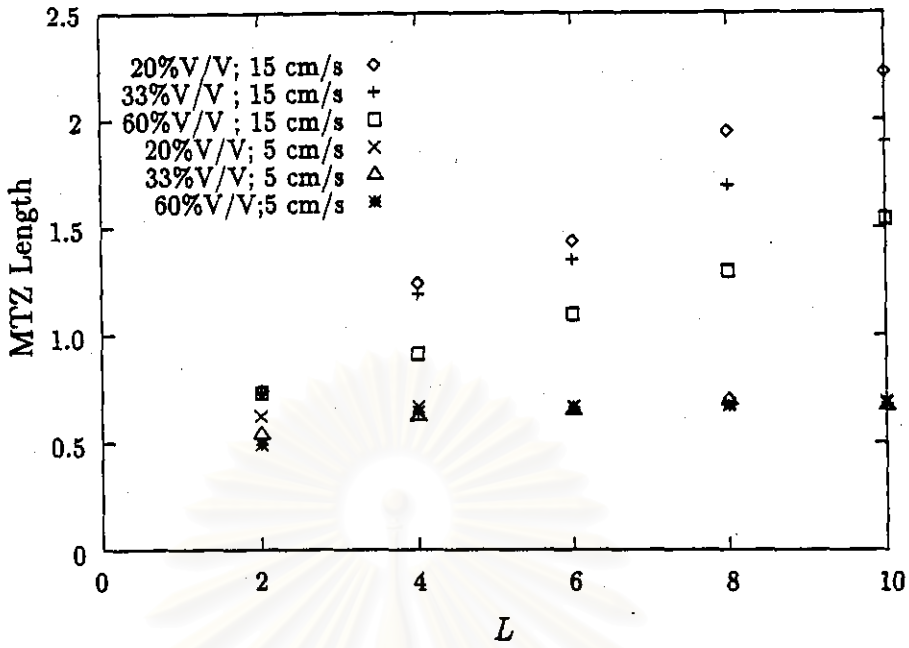

Figure 4.17: An experimental MTZ length

are equal for all bed lengths. The constant MTZ length as propagating through the YAO bed corresponds with the constant shape of the profile. Under the circumstances, the MTZ length is equal to 0.65 cm approximately. In comparison with the experiments with the velocity of 15 cm/s, the MTZ length depends on both feed concentration and the velocity of gas.

The finite rate of adsorption causes the existance of the MTZ in this system. The rate of adsorption ought to be limited by either the mass transfer across the external film or that in the pores. With the properties of the gas mixture, configuration of the adsorber and the operating condition, the mass transfer coefficient across the external film can be determined independently by the use of equation 2.15, as shown in Figure 4.18.

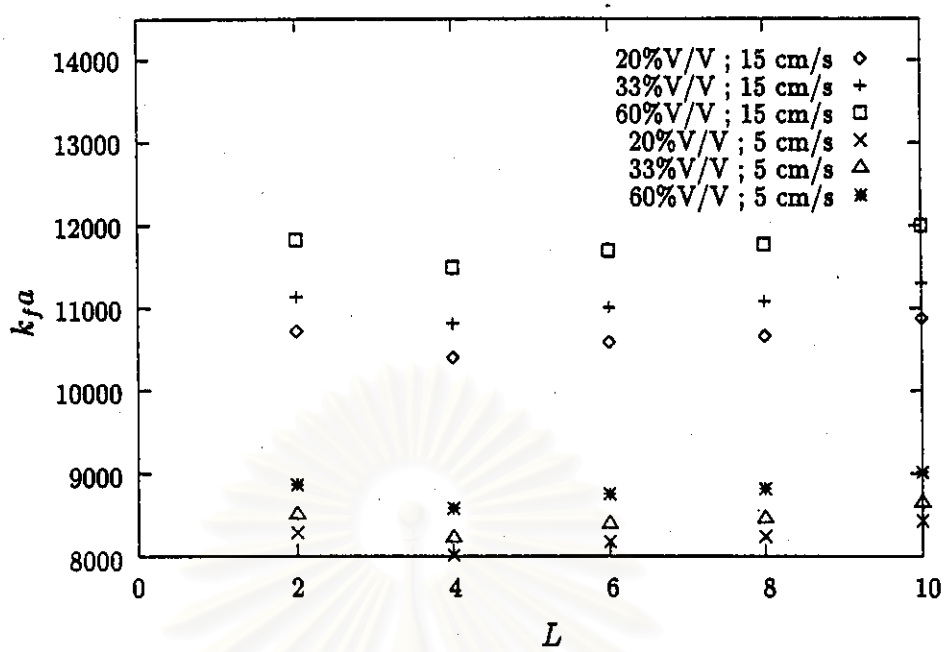

Figure 4.18: The external fluid film mass transfer coefficient

For the high velocity, the thickness of the film is reduced, thus the mass transfer coefficient is higher than that for the low velocity.

For the mass transfer in the pores of YAO, the mass transfer coefficient can be determined from the corresponding MTZ data [15, 9]. The pore mass transfer coefficients of all experiments are shown in Figure 4.19. The calculation method are represent in Appendix A.

Based on the MTZ lengths, the mass transfer coefficients for a short column is higher than that for a long column. This trend is not resonable because the pore mass transfer coefficient must not depend on the column length. For the velocity of 15 cm/s under which the shape of the profile expands with an increase in the MTZ data, the pore mass transfer coefficient decreases and tends to approach a

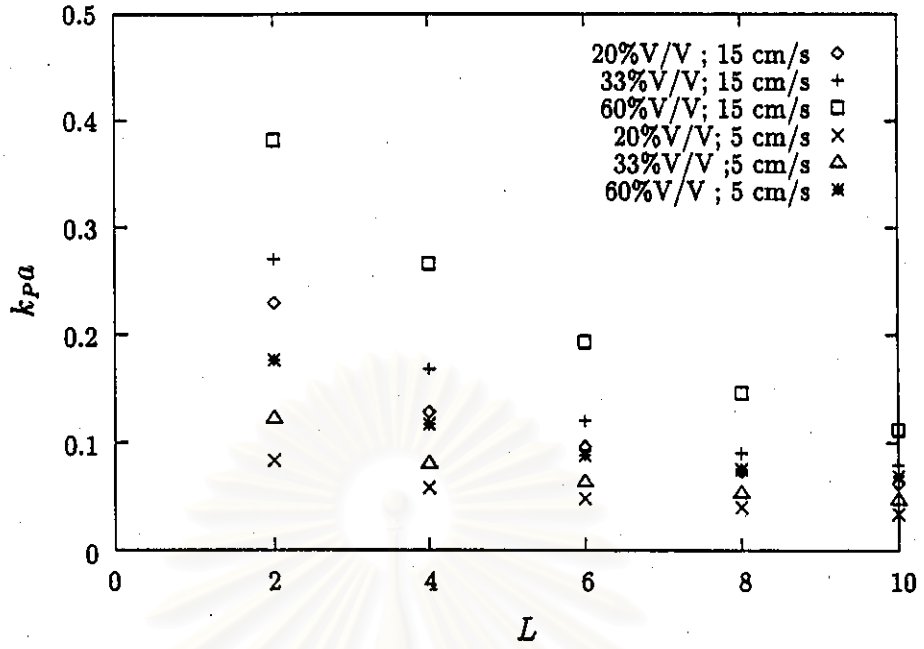

Figure 4.19: The pore mass transfer coefficient

certain values. With the velocity of 5 cm/s under which the shape of the profile is almost constant, the trend of the pore mass transfer coefficient is slightly decrease with an increase in column length.

These results demonstrate that the calculation under constant pattern condition give more reliable mass transfer data. In addition, although the shape of the profile is constant, the approximate mass transfer coefficient has to be obtained from the MTZ data with sufficient residence time.

In comparison the rates of mass transfer between across the external film and within the pore, the coefficients of the external film are much higher than that of the pores, even with the low velocity. Consequently, the rate of adsorption of acetylene on YAO is controlled by the pore diffusion.